communications physics

Article

https://doi.org/10.1038/s42005-024-01782-8

Toroidal phase topologies within paraxial laser beams

Check for updates

Jinzhan Zhong [1,2], Houan Teng[1] & Qiwen Zhan [1,2,3]

Control of topologies in structured light fields with multi-degrees of freedom integrates fundamental optical physics and topological invariance. Beyond the simple phase vortex, three-dimensional (3D) topological singularities and related nonsingular textures have recently gained significant interest. Here, we experimentally demonstrate the creation of a family of toroidal phase topologies within paraxial laser beams. By employing single two-dimensional (2D) phase control, we generate propagating 3D topological textures, effectively embodying the topological configuration of a four-dimensional (4D) parameter space. The resulting light fields exhibit amplitude isosurfaces of toroidal vortices and hopfionic phase textures, both controlled by topological charges. The ability to prepare scalar phase textures of light offers new insights into the high-dimensional control of complex structured textures and may find significant applications in light-matter interactions, optical manipulation, and optical information encoding.

The interplay between non-trivial topologies and physical fields lies at the heart of current research. In this context, much interest has focused on the physical properties related to knot theory[1]. There is a growing realization that the knot physics are essential parts of many physical processes, including liquid crystals[2,3], classical and quantum fluids[4,5], magnetic systems[6,7], quantum fields[8,9] and acoustic waves[10,11]. In optics, the customized structured light field with muti-degrees of freedom is an excellent experimentally accessible platform for studying general knot topologies[12–14]. Deriving from the idea of Lord Kelvin's knotted vortex atoms hypothesis, the interest in combining the concept of singular optics with knot topologies has lasted for quite a long time[15,16]. For instance, beyond single singularity in a 2D plane, the trajectory of phase or polarization singularities embedded in 3D light fields can be woven into knots and links[17–20]. The entire light fields are twisted everywhere to match the topological structures as the core, and thus exhibit topological protection against perturbation[21,22]. In addition, topological light fields with controllable topological invariants inspire research interests due to their potential application in optical encoding and communication[20,23,24].

As a trivial structure in the knot family, the core of toroidal vortices is the simplest knot mathematically. Well-known examples of toroidal vortices in nature are smoke rings from active volcanoes and bubble rings from dolphins. Ever since Tait's smoke ring experiment, the creation of toroidal vortices has been extremely attractive as subject of study in fluid mechanics[25]. Recently, two types of toroidal pulses in optics have attracted wide attention[26]. One is spatiotemporal toroidal vortices, in which conformal mapping transforms a spatiotemporal vortex with transverse orbital angular momentum to a toroidal topology[27–29]. The symmetrical toroidal vortices have been extended to the photon conch with chirality[30]. Another one is the toroidal light pulses, electric (or magnetic) field lines forming a torus topology[31–33]. Indeed, the formation and topological stability of these topological configurations depend on precise spatiotemporal shaping.

Topological objects that are closely related to toroidal topologies and have particle-like properties are hopfions[34,35]. The Hopf fibration establishes the mapping between a unit-sphere in 4D space (3-sphere S^3) and a unit sphere in 3D space (2-sphere S^2). For a point in unit 2-sphere, its preimage corresponds to a circle in 4D real space R^4. The investigation of the 3-sphere can be projected into the familiar 3D real space with preserving the topological properties. Particle-like structured lights with elegant topological textures such as optical skyrmions and hopfions attracted widespread interests[36]. Structured vector beams with spatially varying polarization are preferentially considered to carry these topologies. Orthogonal polarization components in space were controlled artificially to form baby skyrmion in 2D transverse plane and hopfions in 3D beams[37]. Three-dimensional skyrmionic hopfions were extended to higher-order cases with relatively complex polarization textures[38,39].

In this work, we theoretically propose and experimentally create a family of toroidal phase topologies within paraxial laser beams. These phase topologies are constructed under the framework of high-dimensional parameter space and stereographic projection. We generate the optical

[1]School of Optical-Electrical and Computer Engineering, University of Shanghai for Science and Technology, Shanghai, 200093, China. [2]Zhangjiang Laboratory, 100 Haike Road, Shanghai, 201204, China. [3]International Institute for Sustainability with Knotted Chiral Meta Matter (WPI-SKCM2), Hiroshima University, Higashihiroshima, Hiroshima, 739-8526, Japan. e-mail: qwzhan@usst.edu.cn

toroidal vortices and related hopfionic phase textures by exploiting single phase modulation. Different from the skyrmionic hopfions constructed with spatial polarization distribution, the proposed topological textures are scalar counterparts formed by spatial phase distribution. The observed phase fibers are attached to the toroidal amplitude isosurface of the light fields. The topological configuration of the phase fibers and the topological invariants of the light field are determined by the topological charges of the toroidal vortices and the axial vortex. These phase topological structures possess characteristics for potential applications in high-dimensional information encoding and light-matter interactions[2,20,23].

Results

High-dimensional space and stereographic projection

Topologically, knotted and linked curve relate to singularities in high-dimensional spaces. Consider a non-constant polynomial with two complex variables u, v that can form a 4D space, the algebraic set consisting of polynomial zeros corresponds to a complex hypersurface. The intersection of the hypersurface with unit 3-sphere S^3 centered at the origin may lead to knotted curve. To establish a connection between the hypersphere and 3D real space, stereographic projection can reduce the spatial dimension and preserve the topology. In this case, one type of projection can be defined as

$$\begin{aligned} u &= \frac{R^2 + z^2 - 1 + 2iz}{R^2 + z^2 + 1} \\ v &= \frac{2Re^{i\phi}}{R^2 + z^2 + 1} \end{aligned} \tag{1}$$

where (R, ϕ, z) are cylindrical coordinates in 3D real space. In fact, the projection functions have inherent topological textures. The zero set of function u is a unit circle centered at the origin of the coordinate. As shown in Fig. 1a, the amplitude isosurface of the function u is a torus, which gradually shrinks to the black ring as the amplitude decreases. The colored arrows reflect the local phase structure in the space. It means that in the $z = 0$ plane, the complex function u contains toroidal phase singularities in real space. It can be directly found the familiar vortex phase from complex function v. Due to the constraint of hypersphere, complex function v also has toroidal amplitude isosurfaces. As illustrated in Fig. 1b, the vortex phase structure is drawn around the inner surface of the torus, with the black singularity line passing through the center of the torus.

Different from the zero set of complex function $f(u, v)=u^m-v^n$ leading to the (m, n) torus knots, here we consider complex function $f(u, v)=uv$ and related topological textures. As displayed in Fig. 1c, the complex function has both toroidal and straight singularity lines. The total phase of the complex function is determined by the toroidal vortices and axial vortex. In toroidal coordinates, the axial vortex will rotate the phase structure around the toroidal isosurface. In contrast to Fig. 1a, the red arrow rotates as the poloidal coordinate changes. In addition, the red arrow wraps round toroidal coordinate once and poloidal coordinate once, thus marking (1, 1) torus knot trajectory in space. All the knots correspond to 2π phase values fill the torus surface, and the spatial rotation relationship between them is determined by the topological charge of the axial vortex. Each pair of knots with different phase values forms a Hopf link, and the axial vortex line passes through the interior of each knot. These key structural features indicate the complex scalar field forming hopfionic phase textures.

Experimental observation of paraxial toroidal vortices

The construction of optical toroidal topologies relies on the above theoretical model. Although the complex function does not satisfy the wave equation, it contains the expected topology. After addition of Gaussian factor, the polynomial function becomes the target physical field. We first design the light field in a 2D transverse plane so that it matches the distribution of the complex scalar function in the $z = 0$ plane, and then propagate it in paraxial conditions to obtain the entire 3D light field. Here we use the Laguerre-Gaussian ($LG_{l,p}$) modes as the orthogonal bases to further decompose the physical field into the topological light field, where l is the azimuthal mode number, p is the radial mode number. For the paraxial toroidal vortices, it can be decomposed into the linear superposition of $LG_{0,0}$ and $LG_{0,1}$ modes, which can be expressed as

$$\begin{aligned} E_{\text{toroidal}}(R, \phi, z, w) &= \alpha LG_{0,0} - \beta LG_{0,1} \\ &= C(R, \phi, z, w)\left[\alpha + \beta\left(\frac{2R^2}{w^2(z)} - 1\right)\exp(-2i\Phi(z))\right] \end{aligned} \tag{2}$$

where α, β are any positive real number and determine the radius of the toroidal vortices, with a radius of $\sqrt{\beta - \alpha/2\beta}w$ in the $z = 0$ plane, $C(R, \phi, z, w)$ is the common term of the two modes, and $\Phi(z)$ is the Gouy phase. Similar to the distribution of the complex function u, Eq. (2) also provides a toroidal vortex phase, although it is not located in a standard torus.

Taking the parameter $\alpha = 1$, $\beta = 2$ as an example, we will illustrate the observation of embedding toroidal vortices into the designed laser beam. To keep the topological configuration in the 3D propagating beam, the modulated light field needs to satisfy both the amplitude and phase

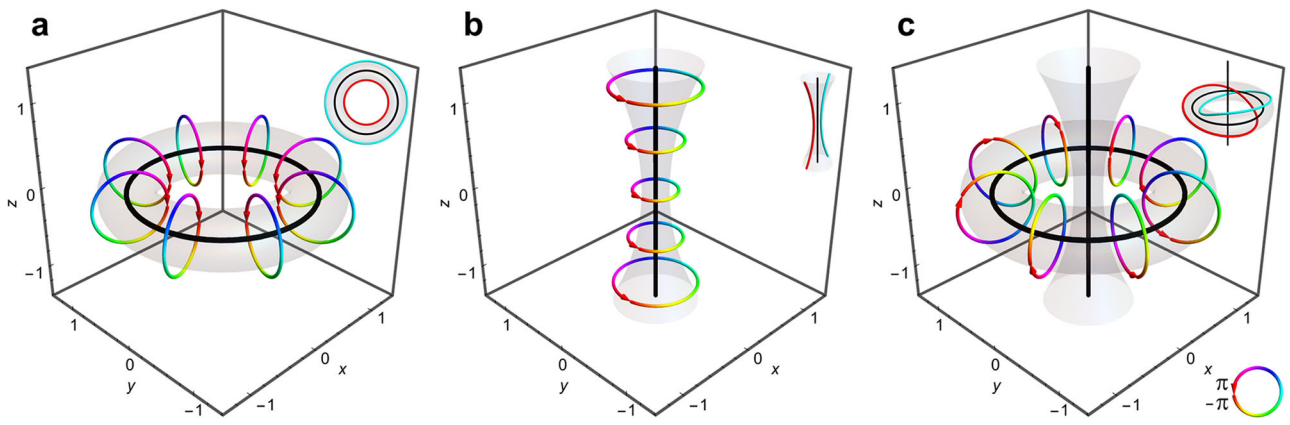

Fig. 1 | Theoretical construction of toroidal phase topologies. a Three-dimensional toroidal amplitude isosurface of the complex function u. The toroidal vortices are represented by a black trajectory, and the local vortex phase structure around the torus is marked with colored arrows. **b** Several local phase structures arising from the vortex phase of the complex function v, with straight vortex line passes through the interior. **c** Hopfionic phase textures embedded in the complex scalar function uv. Local colored arrows rotate due to axial vortices, the circular trajectory formed by the end of the arrow is shown in the illustration. The isovalue of the 3D surfaces is set to 0.3, and the colored curves in the illustration represent the phase fibers formed on the torus.

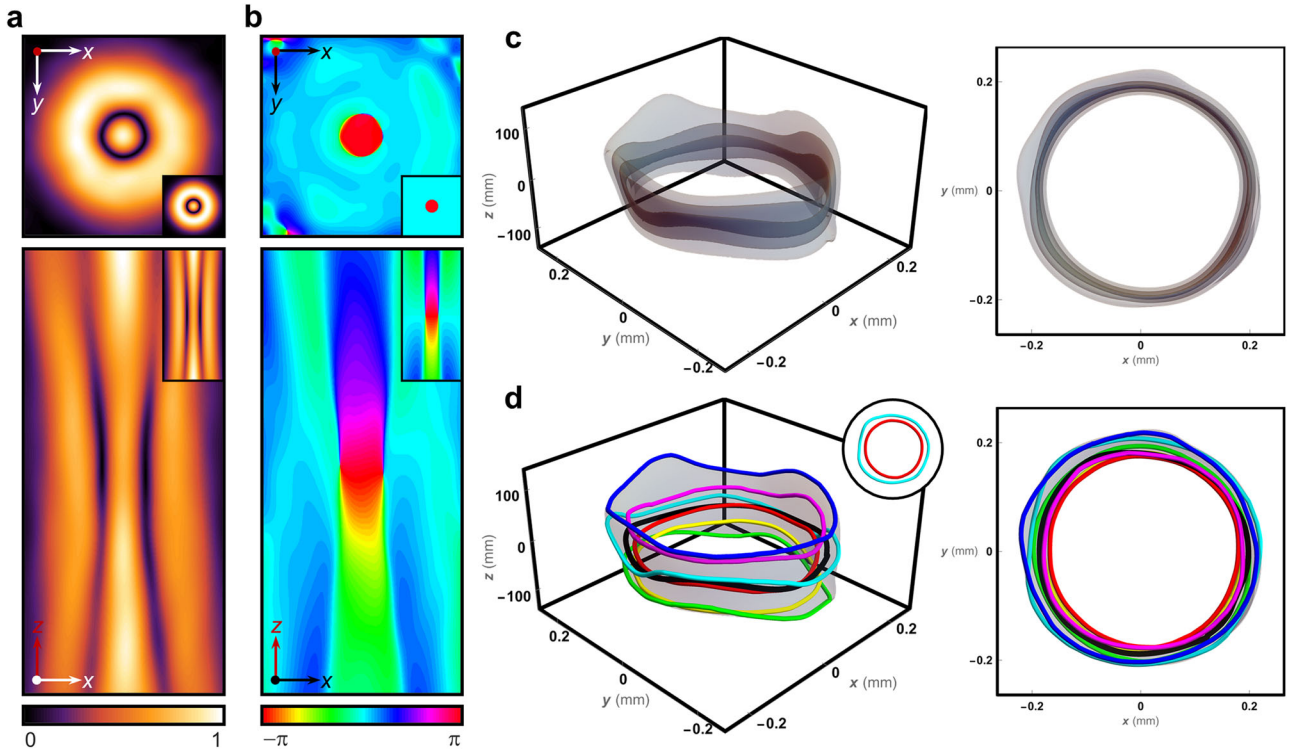

Fig. 2 | Amplitude and phase information of an experimentally generated paraxial toroidal vortices. a Amplitude and **b**, phase profiles of the beam in the transverse (*x*-*y*) and longitudinal (*x*-*z*) planes, longitudinal phase vortices indicate the position of the toroidal vortices. The directional arrows also indicate the beam sizes, which represent 0.4 mm in *x*, *y* direction and 80 mm in *z* direction. Insets show the corresponding simulated profiles. **c** 3D amplitude isosurafces of the paraxial toroidal vortices in different views, the isovalues of the three surfaces are 0.13, 0.08, and 0.03 respectively. **d** The colored curves denote 3D phase fibers on the torus surface, the phase interval is π/3, and the black ring marks the trajectory of the paraxial toroidal vortices.

distributions of Eq. (2). Experimentally, the desired complex field is encoded as a phase-only pattern, which is loaded to a spatial light modulator to shape the paraxial beam. The paraxial toroidal vortices can be obtained by imaging with a 4*f* system and filtering in its focal plane. To observe the spatial trajectory and phase textures of the toroidal vortices, we use the interferometry based on digital holography[40]. Details of experimental setup and light field reconstruction are given in the Methods. From the off-axis hologram recorded in the experiment, the amplitude and phase profiles of the beam in the *x*-*y* plane can be reconstructed, as shown in Fig. 2a, b. It can be found that there is a phase step at the corresponding position of the toroidal darkness in the beam. The light fields in *x*-*z* section visualize the phase singularities of the toroidal vortices clearly. Due to the rotational symmetry of the toroidal vortices, it has the same profile in *y*-*z* section. The full-field measurement reveals the 3D amplitude isosurfaces of the toroidal vortices, as visualized in Fig. 2c. Translucency effect is used to distinguish surfaces formed by different amplitude values. In addition, the phase fibers on the isosurface and the vortex core are visualized in Fig. 2d. Toroidal phase fibers with different phase values are not linked to each other.

Experimental observation of paraxial hopfionic phase textures

Following the theory model of hopfionic phase textures, we consider both toroidal vortices and a straight vortex line. The product of the complex function $f(u, v)=uv^l$ and the Gaussian factor in the $z=0$ plane can be decomposed as the superposition of $\mathrm{LG}_{l,0}$ and $\mathrm{LG}_{l,1}$ modes. which can be expressed as

$$E_{\mathrm{hopfions}}(R,\phi,z,w) = \alpha \mathrm{LG}_{l,0} - \beta \mathrm{LG}_{l,1} \propto \exp(\mathrm{i}\varphi_t)\exp(\mathrm{i}l\varphi_p) \quad (3)$$

where φ_t and φ_p are the azimuth angle in the toroidal and poloidal plane respectively. In this form, the twisted phase of the light field is the sum of the toroidal vortices and straight vortex. Using the same experimental method, we observed the phase textures when the topological charge l is 1. Figure 3a, b visualize the amplitude and phase profiles of the beam in the transverse and longitudinal planes. It can be clearly seen that the dark core and the toroidal darkness both exist in the transverse profile of the beam. Note that, in the longitudinal distribution, although the amplitude distribution retains rotational symmetry, the phase distribution changes with the observed plane due to the transverse vortex phase. The amplitude isosurfaces shown in Fig. 3c demonstrate the presence of toroidal vortices in the beam as well. The experimentally determined hopfionic phase textures are shown in Fig. 3d. The reconstructed phase fibers are well attached to the amplitude isosurface, and all phase fibers wrap round the central hole and the toroidal vortices in the same manner. Thus, each pair of phase fibers is linked to each other. As an example, the inset of Fig. 3d shows a Hopf link formed by phase fibers with 0 and π phase values.

High-order hopfionic phase textures

According to Eq. (3), we extend the paraxial hopfionic phase textures to the higher-order case. Since the beam shaping in the experiment is located in the 2D transverse plane, it is relatively easy to achieve the high-dimensional control of the transverse vortex structures. Although higher-order vortices tend to exhibit instability under perturbations and thus split into multiple singly charged vortices, such imperfections occur in the center of the beam and do not affect the observation of higher-order hopfionic phase textures on the torus. For second and third order phase hopfions, the experimentally observed amplitude torus are shown in Fig. 4a, d. It can be seen that the radius of the toroidal vortices increases slightly with the topological charge. The experimentally extracted higher-order phase fibers are visualized in Fig. 4b, e, which clearly shows the topological features of the phase hopfions. The points on the phase fiber always pass through the internal circle of the torus l times and around the center of the torus once, thus marking $(1, l)$ torus knot trajectory. This topological feature is exemplarily visualized in Fig. 4c, f with only two phase fibers.

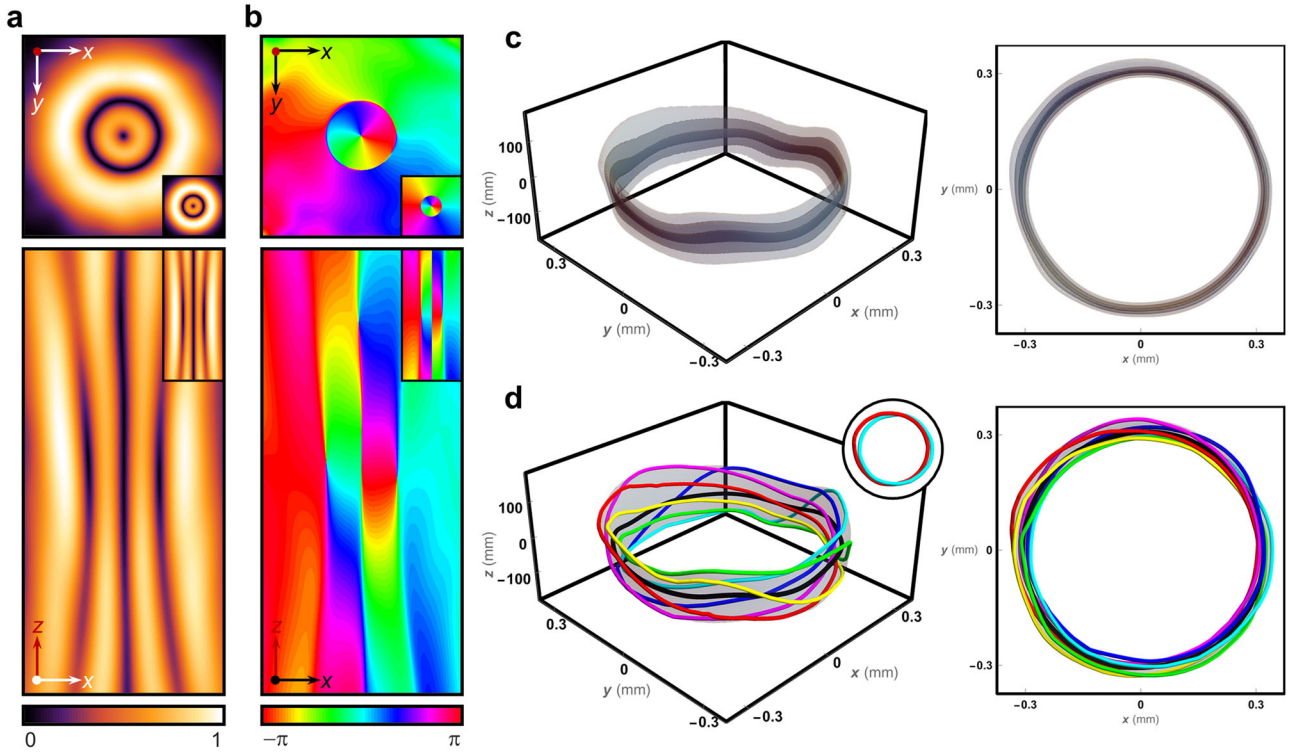

Fig. 3 | Amplitude and phase information of an experimentally generated phase hopfions. a Amplitude and **b**, phase profiles of the beam in the transverse (*x*-*y*) and longitudinal (*x*-*z*) planes. The directional arrows also indicate the beam sizes, which represent 0.4 mm in *x*, *y* direction and 80 mm in *z* direction. Insets show the corresponding simulated profiles. **c** 3D amplitude isosurfaces of the phase hopfions in different views, the isovalues of the three surfaces are 0.13, 0.08, and 0.03 respectively. **d** The colored curves denote 3D phase fibers on the torus surface, the phase interval is π/3, and the black ring marks the trajectory of the paraxial toroidal vortices. Insets show the Hopf link formed by two phase fibers.

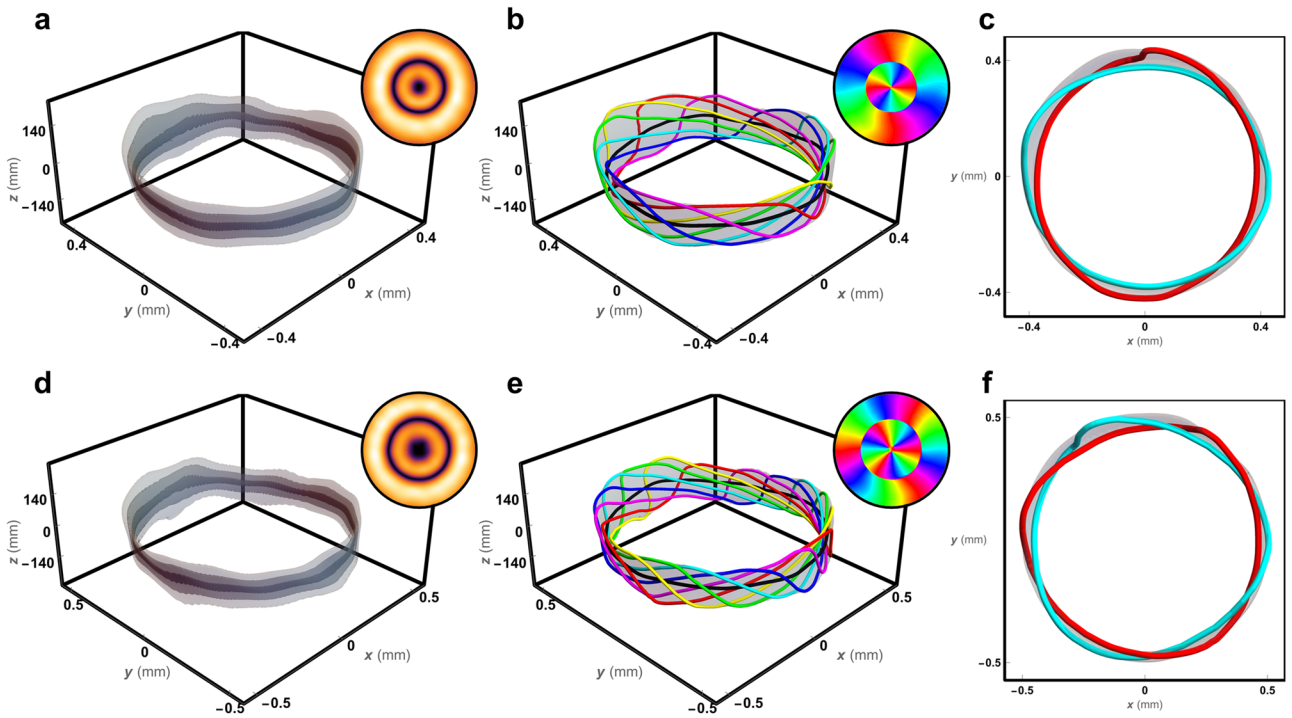

Fig. 4 | Visualizing the topology of high-order hopfionic phase texture. a, d 3D amplitude isosurfaces of second and third order phase hopfions, insets show the amplitude profiles in the $z = 0$ plane. **b**, **e** The experimentally extracted 3D phase fibers of the high-order hopfions, insets show the phase profiles in the $z = 0$ plane. The phase interval is π/3, and the black ring marks the trajectory of the paraxial toroidal vortices. **c**, **f** The Hopf link formed by two phase fibers with 0 and π phase values.

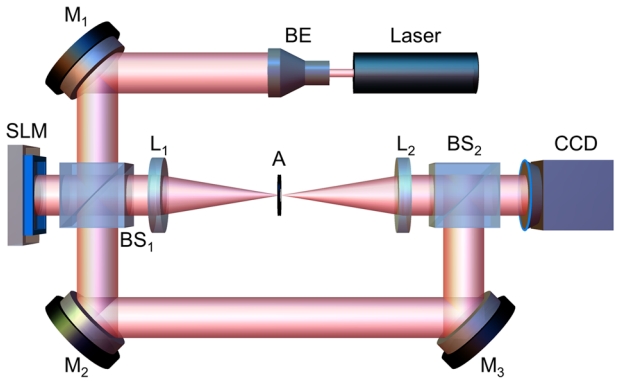

Fig. 5 | Experimental setup. BE Beam expander, M_1-M_3 Mirror, SLM Spatial light modulator, L_1, L_2 Lens, A Aperture, BS_1, BS_2 Beam splitter, CCD Charge coupled device.

Discussions

In the above experiments, the high-order hopfionic phase textures with topological charges $l > 1$ are generated. Thanks to the precise control of the higher-order transverse vortex structures and their acceptable slight splitting (see insets in Fig. 4b, e), the phase textures are very stable for experimental observation. However, singly charged toroidal vortices limit the topological configuration of the phase fibers. For the even-order paraxial toroidal vortices, it has a uniform phase profile in the $z = 0$ plane, and the longitudinal singularity splitting cannot be ignored in the experiment. Therefore, the generation of high-order toroidal vortices is the key to expanding the configuration of phase fibers, but also presents a great experimental challenge.

Recently, optical vortex knots and links under tight focusing conditions have been explored both theoretically and experimentally[41,42], where topological structures can be reduced to the order of wavelength in 3D space. It might be interesting to combine these techniques with the hopfionic phase textures. In addition to the spatial aspect ratio, this may promote high-order toroidal vortices and more complex phase texture structures.

In summary, we propose and demonstrate a class of toroidal phase topologies within paraxial laser beams. The construction of 3D phase topologies requires only single 2D phase modulation. Through the use of high-dimensional space and stereographic projection, we demonstrate the generation of paraxial toroidal vortices and related hopfionic phase textures. In addition, we perform full-field reconstruction of the phase fibers, each pair of equiphase lines is linked for the phase hopfions. The topological structure of the equiphase lines is completely determined by the topological charges of the toroidal vortices and the axial vortex. More fundamentally, the fine phase textures demonstrate the potential for topological control in paraxial beams. These topological textures associated with singularities may be of interest in topological excitation in material and high-dimensional information encoding[2,20,23].

Methods

Experimental setup

The experimental setup used to generate and characterize toroidal phase topologies is shown in Fig. 5. The linearly polarized beam emitted from a He–Ne laser (632.8 nm) is expanded by a beam expander (BE) and then sent to a beam splitter (BS_1) dividing into two beams. The transmitted one is a reference beam for interference. The reflected one is modulated by a reflective spatial light modulator (SLM), where the designed phase-only pattern is controlled by a computer. A weighted blazed grating transfers the desired amplitude and phase information to the first diffraction order of the beam. The modulated beam is then imaged by a 4*f* system consisting of lenses L_1 and L_2, and the first diffraction order is filtered by an aperture (A). After the 4*f* system, the desired toroidal phase topologies are obtained. Finally, the topological light field and reference light are interfered by adjusting the mirror (M) and the beam splitter (BS_2), and the interference pattern is recorded by a charge coupled device (CCD).

Reconstruction of 3D topological structures

The digital hologram recorded in the experiment embodies the 3D topological information of the full-field. By utilizing the digital holography and the angular spectrum relation, we can get the 3D complex amplitude information of the target volume. For the entire reconstructed volume, we divide it into 201 transverse planes in the range of z to investigate the complex amplitude profiles. According to these data and using the isosurface extractor, the toroidal amplitude surface can be obtained. The challenge for the reconstruction of complex phase fibers goes beyond the trajectory of knotted singularities. Our method is suitable for phase textures and singularity structures. Based on the triangulation data of 3D amplitude and phase isosurfaces, we extracted the intersection lines of isosurfaces by using an algorithm developed in-house, thus ensuring the visualization of phase textures on specific amplitude isosurface. The black singularity lines are extracted from the zero isosurfaces of the real and imaginary parts of the complex field.

Data availability

The data that support the findings of this study are available from the corresponding author upon reasonable request.

Code availability

The code used for the data analysis is available from the corresponding author upon reasonable request.

Received: 3 June 2024; Accepted: 16 August 2024;
Published online: 24 August 2024

References

1. Kauffman, L. H. *Knots and Physics* (World Scientific Publishing, 2001).
2. Smalyukh, I. I., Lansac, Y., Clark, N. A. & Trivedi, R. P. Three-dimensional structure and multistable optical switching of triple-twisted particle-like excitations in anisotropic fluids. *Nat. Mater.* **9**, 139–145 (2010).
3. Tai, J.-S. B. & Smalyukh, I. I. Three-dimensional crystals of adaptive knots. *Science* **365**, 1449–1453 (2019).
4. Kleckner, D. & Irvine, W. T. M. Creation and dynamics of knotted vortices. *Nat. Phys.* **9**, 253–258 (2013).
5. Kleckner, D., Kauffman, L. H. & Irvine, W. T. M. How superfluid vortex knots untie. *Nat. Phys.* **12**, 650–655 (2016).
6. Sutcliffe, P. Skyrmion Knots in Frustrated Magnets. *Phys. Rev. Lett.* **118**, 247203 (2017).
7. Zheng, F. et al. Hopfion rings in a cubic chiral magnet. *Nature* **623**, 718–723 (2023).
8. Hall, D. S. et al. Tying quantum knots. *Nat. Phys.* **12**, 478–483 (2016).
9. Ollikainen, T., Blinova, A., Möttönen, M. & Hall, D. S. Decay of a Quantum Knot. *Phys. Rev. Lett.* **123**, 163003 (2019).
10. Zhang, H. et al. Creation of acoustic vortex knots. *Nat. Commun.* **11**, 3956 (2020).
11. Muelas-Hurtado, R. D. et al. Observation of Polarization Singularities and Topological Textures in Sound Waves. *Phys. Rev. Lett.* **129**, 204301 (2022).
12. Forbes, A., de Oliveira, M. & Dennis, M. R. Structured light. *Nat. Photonics* **15**, 253–262 (2021).
13. He, C., Shen, Y. & Forbes, A. Towards higher-dimensional structured light. *Light Sci. Appl.* **11**, 205 (2022).
14. Zhan, Q. Spatiotemporal sculpturing of light: a tutorial. *Adv. Opt. Photon.* **16**, 163–228 (2024).
15. Dennis, M. R., O'Holleran, K. & Padgett, M. J. In *Progress in Optics* Vol. 53 293-363 (Elsevier, 2009).
16. Berry, M. V. & Dennis, M. R. Knotted and linked phase singularities in monochromatic waves. *Proc. R. Soc. A* **457**, 2251–2263 (2001).

17. Dennis, M. R., King, R. P., Jack, B., O'Holleran, K. & Padgett, M. J. Isolated optical vortex knots. *Nat. Phys.* **6**, 118–121 (2010).
18. Zhong, J. et al. Observation of optical vortex knots and links associated with topological charge. *Opt. Express* **29**, 38849–38857 (2021).
19. Larocque, H. et al. Reconstructing the topology of optical polarization knots. *Nat. Phys.* **14**, 1079–1082 (2018).
20. Larocque, H. et al. Optical framed knots as information carriers. *Nat. Commun.* **11**, 5119 (2020).
21. Dehghan, N., D'Errico, A., Jaouni, T. & Karimi, E. Effects of aberrations on 3D optical topologies. *Commun. Phys.* **6**, 357 (2023).
22. Pires, D. G., Tsvetkov, D., Chandra, N. & Litchinitser, N. M. Knots of Darkness in Atmospheric Turbulence. arXiv:2401.12306 (2024).
23. Kong, L.-J. et al. High capacity topological coding based on nested vortex knots and links. *Nat. Commun.* **13**, 2705 (2022).
24. Wan, Z., Wang, H., Liu, Q., Fu, X. & Shen, Y. Ultra-Degree-of-Freedom Structured Light for Ultracapacity Information Carriers. *ACS Photonics* **10**, 2149–2164 (2023).
25. Akhmetov, D. G. *Vortex rings* (Springer Science & Business Media, 2009).
26. Cardano, F. & Marrucci, L. Smoke rings of light. *Nat. Photonics* **16**, 476–477 (2022).
27. Wan, C., Cao, Q., Chen, J., Chong, A. & Zhan, Q. Toroidal vortices of light. *Nat. Photonics* **16**, 519–522 (2022).
28. Wan, C., Shen, Y., Chong, A. & Zhan, Q. Scalar optical hopfions. *eLight* **2**, 22 (2022).
29. Zhong, J., Wan, C. & Zhan, Q. Optical Twisted Phase Strips. *ACS Photonics* **10**, 3384–3389 (2023).
30. Chen, W. et al. Observation of Chiral Symmetry Breaking in Toroidal Vortices of Light. *Phys. Rev. Lett.* **132**, 153801 (2024).
31. Shen, Y., Hou, Y., Papasimakis, N. & Zheludev, N. I. Supertoroidal light pulses as electromagnetic skyrmions propagating in free space. *Nat. Commun.* **12**, 5891 (2021).
32. Zdagkas, A. et al. Observation of toroidal pulses of light. *Nat. Photonics* **16**, 523–528 (2022).
33. Shen, Y., Papasimakis, N. & Zheludev, N. I. Nondiffracting supertoroidal pulses and optical "Kármán vortex streets". *Nat. Commun.* **15**, 4863 (2024).
34. Hopf, H. Über die Abbildungen der dreidimensionalen Sphäre auf die Kugelfläche. *Math. Ann.* **104**, 637–665 (1931).
35. Lyons, D. W. An Elementary Introduction to the Hopf Fibration. *Math. Mag.* **76**, 87–98 (2003).
36. Shen, Y. et al. Optical skyrmions and other topological quasiparticles of light. *Nat. Photonics* **18**, 15–25 (2024).
37. Sugic, D. et al. Particle-like topologies in light. *Nat. Commun.* **12**, 6785 (2021).
38. Shen, Y. et al. Topological transformation and free-space transport of photonic hopfions. *Adv. Photonics* **5**, 015001 (2023).
39. Ehrmanntraut, D. et al. Optical second-order skyrmionic hopfion. *Optica* **10**, 725–731 (2023).
40. Zhong, J. et al. Reconstructing the topology of optical vortex lines with single-shot measurement. *Appl. Phys. Lett.* **119**, 161102 (2021).
41. Sugic, D. & Dennis, M. R. Singular knot bundle in light. *J. Opt. Soc. Am. A* **35**, 1987–1999 (2018).
42. Herrera, I., Mojica-Casique, C. A. & Quinto-Su, P. A. Experimental Realization of a Wavelength-Sized Optical-Vortex Knot. *Phys. Rev. Appl.* **17**, 064026 (2022).

Acknowledgements

We acknowledge financial support from the National Natural Science Foundation of China (NSFC) (92050202, 12304367), the Shanghai Rising-Star Program (23YF1415800), and the Shanghai Post-doctoral Excellence Program (2023533).

Author contributions

J.Z. and Q.Z. proposed the original idea and initiated this project. J.Z. completed the theory and simulations. J.Z. and H.T. performed the experiments and analyzed the data. Q.Z. supervised the project. All authors contributed to the discussion and writing of the manuscript.

Competing interests

The authors declare no competing interests.

Additional information

Correspondence and requests for materials should be addressed to Qiwen Zhan.

Peer review information *Communications Physics* thanks Yijie Shen, and Xiangdong Zhang for their contribution to the peer review of this work.